Guided-to-Leaky Mode Transition in Uniaxial Optical Slab Waveguides

Lluís Torner, *Member, IEEE,* Jaume Recolons, and Juan P. Torres, *Student Member, IEEE*

***Abstract*—The guided-to-leaky hybrid mode transition in slab optical waveguides made on uniaxial crystals such as $LiNbO_3$ or $LiTaO_3$ is analyzed. Two different guided-to-leaky transitions have been identified, namely the *ordinary cutoff* and the *extraordinary cutoff,* which occur when considering negative and positive birefringent materials, respectively. Analytical but transcendental expressions have been obtained, yielding the critical optical axis orientation, relative to the waveguide axis, above which the totally guided hybrid modes become leaky. The results indicate that the value of the critical orientation strongly depends on the waveguide parameters. The possibility of tuning this critical orientation to a desired value through the waveguide parameters is discussed.**

I. Introduction

INTEGRATED optical technology typically employs uniaxial dielectric crystalline materials, such as lithium niobate ($LiNbO_3$) and lithium tantalate ($LiTaO_3$), to obtain low loss optical waveguides. Several waveguide fabrication techniques have been extensively developed in past years and, as a result, the involved technology has become mature [1]. Modulators, switches, polarization controllers, filters, and correlators, among other high-performance devices for signal processing, signal routing and sensing, have been demonstrated in integrated form [2], [3]. Most of these devices are based on the excellent electrooptic and acoustooptical properties of $LiNbO_3$ and $LiTaO_3$. Crystal anisotropy plays also a very important role in many devices, for instance to obtain TE-TM conversion or to optimize phase-matching conditions for second-harmonic generation and other nonlinear parameteric interactions, but it is the central point for the anisotropy-based cutoff devices [4].

The principle of operation of the anisotropy-based cutoff devices is the passive as well as electrooptically induced guided-to-radiated mode conversion. Light-intensity (cutoff or mode excitation) modulators [5] and passive TE-pass [6] or TM-pass [7] polarizers belong to this category of optical devices. With a few exceptions [8], [9], in most cases the guided-to-radiated mode conversion between the TE and the TM modes, which propagate in birefringent waveguides when the propagation direction is parallel or perpendicular to the crystal optical axis, is considered and exploited [10]–[14]. However, with the exception of the former symmetric configurations, all the modes supported by a slab waveguide made on birefringent materials are of the hybrid type, with the six field components. In addition to the well-known totally guided modes, such waveguides suppport the so-called leaky modes. These are leaky guided modes, in contrast to their leaky unguided counterparts which occur in the isotropic case [15]. They are always lossy and energy leakage outside the guiding region.

Totally guided modes as well as leaky modes guided by uniaxial thin dielectric films have been extensively studied since the early days of integrated optics, so now the main features concerning guiding properties are well established [16]–[20]. In particular, leakage losses have been experimentally measured [21] and theoretically calculated [22]–[24] for a $Ti:LiNbO_3$ waveguide, and extensive calculations on the dispersion properties of totally guided modes as a function of the optical axis orientation, relative to the waveguide axis, have been reported [25]. On the contrary, to the best of our knowledge, the critical orientation at which the totally guided modes become leaky has never been analyzed. Our aim here is to address this point. Our goal is to identify the conditions for the guided-to-leaky mode transition (GLMT) to occur, for the common $LiNbO_3$ and $LiTaO_3$-based waveguiding structures, and to investigate the dependence on the waveguide governing parameters of the critical optical axis orientation at which the GLMT takes place. Ultimately, we show that the GLMT exhibits a potential interest for switching applications.

This paper is organized as follows. Section II contains the background of our approach. It is devoted to the introduction of the waveguide configuration we will deal with and to a brief revision of the different type of possible guided modes. In Section III the eigenvalue equation for hybrid guided modes is obtained using the characteristic-matrix approach, and in Section IV we discuss the properties of these modes that are relevant to the GLMT. In Section V we focus on the guided-to-leaky hybrid mode transition. Two different situations are identified, namely the *ordinary cutoff* and the *extraordinary cutoff,* and the expressions giving the value of the critical optical axis orientation at which the GLMT takes place are obtained. Section VI concerns the possibility of tuning the value of this critical orientation through the waveguide parameters. Finally, in Section VII we emphasize our main results.

II. General Modal Properties

The optical waveguide we consider here is shown in Fig. 1. The cover is an isotropic material with refractive index n_c, whereas the guiding layer and the substrate are uniaxial

Manuscript received May 5, 1992; revised November 2, 1992. This work was supported by the Comisión Interministerial de Ciencia y Tecnología of the Spanish Government under grants PT89-0178 and TIC92-0094-C02-02.

The authors are with the Polytechnic University of Catalonia, Department of Signal Theory and Communications, 08080 Barcelona, Spain.

IEEE Log Number 9209997.

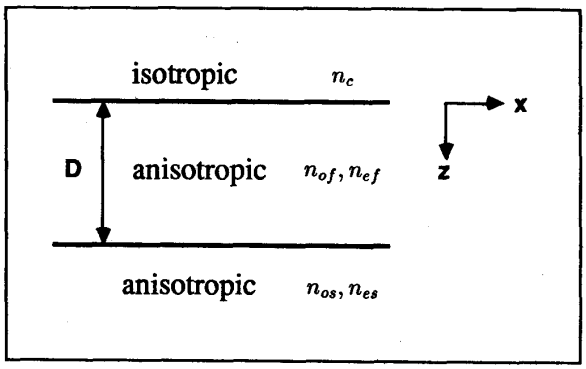

Fig. 1. Schematic of the waveguide structure.

materials. The substrate is homogeneous, whereas the guiding film can be either homogeneous or have an inhomogeneous refractive index profile. In the first case D is the film thickness and in the second one it stands for the characteristic depth of the refractive index profile. We consider a geometry in which the crystal optical axes ($\hat{c}$) are placed in the waveguide plane forming an angle θ with the waveguide axis, and an identical orientation in both substrate and film has been taken. The propagation direction is taken along the x-axis and a time-harmonic dependence has been assumed, so that the fields at any point have the form $\exp[j(\beta x - \omega t)]$, with β being the propagation constant.

In the coordinate system that coincides with the principal axes of the uniaxial crystals (X, Y, Z), the relative dielectric tensor is diagonal and takes the form

$$[\epsilon_r]_{XYZ} = \begin{pmatrix} n_o^2 & & \\ & n_o^2 & \\ & & n_e^2 \end{pmatrix} \tag{1}$$

where n_o and n_e are the ordinary and the extraordinary refractive indices of the material, respectively. For an arbitrary orientation of the optical axes, the dielectric tensor is obtained by application of the appropriate rotation operator to (1). For the orientation considered here one gets a symmetric tensor whose nonvanishing elements write

$$\begin{aligned} \epsilon_{xx} &= n_o^2 \sin^2\theta + n_e^2 \cos^2\theta \\ \epsilon_{yy} &= n_o^2 \cos^2\theta + n_e^2 \sin^2\theta \\ \epsilon_{zz} &= n_o^2 \\ \epsilon_{xy} &= (n_e^2 - n_o^2) \sin\theta \cos\theta \end{aligned} \tag{2}$$

In general, a waveguide such as the former one can only support hybrid modes, with the six field components. In the limiting cases $\theta = 0°$ (X, Y-cut; Z-propagating) and $\theta = 90°$ (X, Y-cut; Y, X-propagating), the allowed guided modes break down in the usual TE and TM sets. The only nonvanishing component of the electric field for TE modes is E_y; therefore the behavior of such modes is governed by ϵ_{yy}. Thus, at $\theta = 0°$, TE modes are affected only by the ordinary refractive index of the different media forming the waveguide; hence such waves are *pure ordinary modes*. Likewise, at $\theta = 90°$, one has $\epsilon_{yy} = n_e^2$, and thus the TE modes are *pure extraordinary modes*. These two types of modes are referred to as o-like modes and e-like modes, respectively.

Concerning TM modes, they have the other two components of the electric field. In the coordinate system used here the predominant component is E_z; hence, the behavior of these waves is basically governed by ϵ_{zz}. At $\theta = 90°$, one has $\epsilon_{xx} = \epsilon_{zz} = n_o^2$; thus at this orientation the TM modes are o-like modes. On the other hand, at $\theta = 0°$, $\epsilon_{xx} = n_e^2$, whereas $\epsilon_{zz} = n_o^2$, so that TM modes are affected by both refractive indices. Nevertheless, as $\epsilon_{zz} = n_o^2$, the TM modes behave as *predominantly ordinary modes*. Such modes are referred to as (o)-like modes.

For an intermediate value of θ, the hybrid guided modes are a superposition of the ordinary and the extraordinary waves propagating in an unbounded uniaxial dielectric medium. In the case of an homogeneous waveguide, the fields in the film are a superposition of two ordinary and two extraordinary plane waves [25]. A particular combination of these waves corresponds to a perfectly guided mode when both ordinary and extraordinary waves are totally reflected at the interfaces between the guiding layer and the surrounding media. Then, outside the guiding region in fields are evanescent and the guided power propagates parallel to the waveguide axis. This is a *totally guided hybrid mode*.

Because the ordinary and the extraordinary waves propagate with different phase velocities, the condition of total reflection at the boundaries cannot always be satisfied for both waves. This means that only one of them will achieve total internal reflection, whereas the other will be only partially reflected. This results in radiation losses. The actual nonstationary guided wave can be approximately described by a hybrid guided mode propagating with attenuation, thus having a complex propagation constant. This is a *leaky guided hybrid mode*.

The relative weight of the ordinary and the extraordinary waves in the hybrid guided mode is dictated by the eigenvalue equation. The hybrid modes which main contribution corresponds to the ordinary or extraordinary waves are referred to as $[o]$-like modes or $[e]$-like modes, respectively. The precise nature of the $[o]$-like and $[e]$-like modes in terms of totally and partially reflected waves has a very strong influence on the loss coefficient of leaky modes [18]–[24], [26]. This nature will also play a crucial role on the GLMT.

According to the former discussion, the critical optical axis orientation we are looking for follows from the eigenvalue equation at the cutoff point for the ordinary or extraordinary waves. Therefore, next we obtain the eigenvalue equation for guided waves, with the help of the characteristic-matrix approach.

III. Characteristic-Matrix Formalism

The key of the formalism runs as follows. Since we are looking for the eigenvalue equation for guided solutions, the fields in the cover and in the substrate must be evanescent. So, they would have the form

$$\vec{E}_c(z) = \vec{E}_c \exp[k_0 \gamma_c z], \qquad z < 0 \tag{3}$$

$$\vec{E}_s(z) = \vec{E}_s \exp[k_0 \gamma_s (D - z)], \qquad z > D \tag{4}$$

These fields must obey the wave equation. In a lossless uniaxial dielectric medium it writes

$$\nabla^2\vec{E} + k_0^2[\epsilon_r]\vec{E} = \nabla(\nabla\cdot\vec{E}) \tag{5}$$

with k_0 being the free-space wave number. In the substrate, taking into account (2), the substitution of (4) into the wave equation leads to two possible solutions for the decay constant γ_s that correspond to the ordinary and extraordinary waves. One gets, respectively

$$\gamma_{os} = [N^2 - n_{os}^2]^{1/2} \tag{6}$$

$$\gamma_{es} = \frac{n_{es}}{n_{es}(\theta)}[N^2 - n_{es}^2(\theta)]^{1/2} \tag{7}$$

where $N \equiv \beta/k_0$ is the effective index and

$$n_{es}(\theta) = \frac{n_{os}n_{es}}{\sqrt{n_{os}^2\sin^2\theta + n_{es}^2\cos^2\theta}} \tag{8}$$

In the isotropic cover these solutions degenerate and one obtains

$$\gamma_c = [N^2 - n_c^2]^{1/2} \tag{9}$$

According to (6) and (7), in the substrate the evanescent fields are a superposition of the ordinary and extraordinary waves, so that (4) becomes

$$\vec{E}_s(z) = \vec{E}_{os}\exp[k_0\gamma_{os}(D-z)] + \vec{E}_{es}\exp[k_0\gamma_{es}(D-z)] \tag{10}$$

The existence of the solutions (6) and (7) implies that all the components of the fields $\vec{E}_{os}$ and $\vec{E}_{es}$ can be expressed in terms of two of them. We have chosen as independent variables the $\hat{y}$ and $\hat{x}$ component sof the electric field associated to the ordinary and extraordinary waves, respectively. Then, the electric field in the substrate can be written as

$$\vec{E}_s(z) = \begin{bmatrix}\Delta_{ox} & 1\\ 1 & \Delta_{ey}\\ \Delta_{oz} & \Delta_{ez}\end{bmatrix}\begin{Bmatrix}E_{os}\exp[k_0\gamma_{os}(D-z)]\\ E_{es}\exp[k_0\gamma_{es}(D-z)]\end{Bmatrix} \tag{11}$$

where, in order to render the expressions in a compact form, a matrix notation has been adopted. The coefficients Δ appearing in the above expressions follow from the wave equation. One gets

$$\Delta_{ox} = -\tan\theta, \qquad \Delta_{ey} = \frac{n_{os}^2}{\gamma_{os}^2}\Delta_{ox} \tag{12}$$

$$\Delta_{oz} = j\frac{N}{\gamma_{os}}\Delta_{ox}, \qquad \Delta_{ez} = j\frac{\gamma_{es}}{\gamma_{os}^2}N \tag{13}$$

In the cover, the double solution (9) gives an expression analogous to (11), but for the TE and the TM field components. One has

$$\vec{E}_c(z) = \begin{bmatrix}0 & 1\\ 1 & 0\\ 0 & -jN/\gamma_c\end{bmatrix}\begin{Bmatrix}E_{oc}\\ E_{ec}\end{Bmatrix}\exp[k_0\gamma_c z] \tag{14}$$

According to the characteristic-matrix formalism, the fields (11) and (14) are continued across the intermediate dielectric medium by means of a characteristic matrix containing the field solutions. Thus, the required boundary conditions on the waveguide dielectric interfaces are verified if the field solutions appearing in the characteristic matrix join with the evanescent fields given by (11) and (14). Following the Berreman approach [27], the characteristic matrix T of a dielectric film of thickness D is defined as

$$\Psi(z=D) = T\Psi(z=0) \tag{15}$$

with $\Psi(z)$ being a four-dimensional array containing the tangential field components. As is customary, we have chosen an ordering criterion in such a way that the transpose of Ψ writes $\Psi^t = (E_x, H_y, E_y, H_x)$. The tangential components of the magnetic field in the substrate and in the cover appearing in Ψ following immediately from (11) and (14) by means of Maxwell equations. One arrives at

$$\vec{H}_s(z) = \frac{1}{j\eta}\begin{bmatrix}\gamma_{os} & \gamma_{es}\Delta_{ey}\\ \tau_{os} & \tau_{es}\\ jN & jN\Delta_{ey}\end{bmatrix}\cdot\begin{Bmatrix}E_{os}\exp[k_0\gamma_{os}(D-z)]\\ E_{es}\exp[k_0\gamma_{es}(D-z)]\end{Bmatrix} \tag{16}$$

$$\vec{H}_c(z) = \frac{1}{j\eta}\begin{bmatrix}-\gamma_c & 0\\ 0 & -n_c^2/\gamma_c\\ jN & 0\end{bmatrix}\cdot\begin{Bmatrix}E_{oc}\\ E_{ec}\end{Bmatrix}\exp[k_0\gamma_c z] \tag{17}$$

Here η is the characteristic impedance of free-space and use has been made of the definitions

$$\tau_{os} = \frac{n_{os}^2}{\gamma_{os}}\Delta_{ox}, \qquad \tau_{es} = \frac{n_{os}^2}{\gamma_{os}^2}\gamma_{es} \tag{18}$$

Substituting (11), (14), (16), and (17) into (15), a homogeneous equation system for E_{os}, E_{es}, E_{oc}, and E_{ec} is obtained, and the condition for having a nontrivial solution is that the determinant of the coefficient matrix vanishes. This condition is the eigenvalue equation. After straightforward manipulation it can be expressed as

$$\begin{aligned}&\tau_{os}[N_{34} - \Delta_{ey}(N_{14} + \gamma_{es}N_{13})] - \Delta_{ox}[\tau_{es}N_{34}\\ &+ \Delta_{ey}(N_{24} + \gamma_{es}N_{23})]\\ &+ [N_{24} + \tau_{es}N_{14} - \gamma_{es}\Delta_{ey}N_{12}]\\ &+ \gamma_{os}[N_{23} + \tau_{es}N_{13} + \Delta_{ey}N_{12}] = 0\end{aligned} \tag{19}$$

where

$$N_{il} = \nu_{io}\nu_{le} - \nu_{ie}\nu_{lo} \tag{20}$$

with

$$\nu_{io} = \Gamma_i\left(T_{i3} + \frac{j}{\eta}\gamma_c T_{i4}\right) \qquad \nu_{ie} = \Gamma_i\left(T_{i1} + \frac{j}{\eta}\frac{n_c^2}{\gamma_c}T_{i2}\right) \tag{21}$$

Here T_{il}, with $i,l = 1-4$, are the elements of the matrix T, and Γ_i has been defined by the formal expression

$$\Gamma_i \equiv -1 + (1 + j\eta)(\delta_{i2} + \delta_{i4}) \tag{22}$$

with δ_{il} being the Kronecker symbol.

The characteristic matrix of a homogeneous uniaxial dielectric film can be analytically calculated by using the 4×4

formalism. The derivation follows a general procedure derived by Vassell [28]. An alternative approach based on the well-known Cayley-Hamilton theorem has been reported more recently by Wöhler *et al.* [29]. When the optical axis lies on the waveguide plane the characteristic matrix is given by a simple expression, which can be found in [26] and [29]. In the case of inhomogeneous structures the characteristic matrix must be obtained with the help of approximate methods or numerical techniques. Here we have used the multilayer staircase technique in which the inhomogeneous region is considered a finite set of thin homogeneous films. Then, the characteristic matrix of the whole structure follows from the product of all the matrices associated to each layer, according to the ordering criterion prescribed in (15).

IV. Hybrid Guided Modes

In this section dicusss the properties of the hybrid guided modes that are relevant to the GLMT. We have considered media with positive and negative birefringence, using in both cases the typical parameters of the $LiNbO_3$ and $LiTaO_3$-based waveguides operating at $\lambda = 632.8$ nm.

First, we are going to deal with a material with negative birefringence, such as $LiNbO_3$. In Fig. 2(a) we have plotted the effective indices of the hybrid modes guided by an homogeneous waveguide with the following parameters

$$G_1: \begin{cases} n_{of} = 2.2946 & n_{ef} = 2.2108 & n_c = 1.0 \\ n_{os} = 2.2866 & n_{es} = 2.2028 & D = 3.0\,\mu\text{m} \end{cases}$$

This is a multimode waveguide, with two modes for each polarization. When $\theta = 0°$ $(\hat{e}||\hat{x})$, G_1 supports the TE_0 and the TE_1 modes, which are o-like modes, together with the TM_0 and TM_1 ones, which are (o)-like modes. Due to the small birefringence of G_1, modes of equal order propagate with very similar effective indices. When θ increases from 0°, these modes become hybrid and some intervals of values of θ appear where the guided modes exhibit very close effective index values, to such an extent that they are almost degenerate. These intervals will be referred to as near-degeneracy regions (NDRs). On the other hand, the first-order modes at $\theta = 0°$ become leaky over a critical θ-value. This is the guided-to-leaky mode transition angle (GLMTA) θ_l for each mode. The lowest order modes, TE_0 and TM_0 at $\theta = 0°$, remain guided for all values of θ. At $\theta = 90°$, the four modes become again TE-TM. In order to identify the hybrid modes, we are using the notation by Knoesen, Gaylord, and Moharam [25]. For instance, the mode which at $\theta = 0°$ is the TE_0 and at $\theta = 90°$ is the TM_0, is denoted as: $[TE_0, TM_0]$. The behavior of the effective index of the allowed hybrid modes as a function of θ is summarized in the diagram in Fig. 2(b). Symbols used in this figure, which is referred to as an $[o]$-$[e]$ diagram, correspond to the above-introduced notation and tilt arrows indicate near-degeneracy regions.

Let us now focus on the $[TE_1, TE_0]$ and the $[TM_1, TE_1]$ modes. In the neighborhood of $\theta = 0°$ these modes evolve with θ as $[e]$-like and $[o]$-like modes, respectively. When θ increases, after the common NDR the roles become inverted, hence the mode $[TM_1, TE_1]$ is an $[e]$-like mode when it

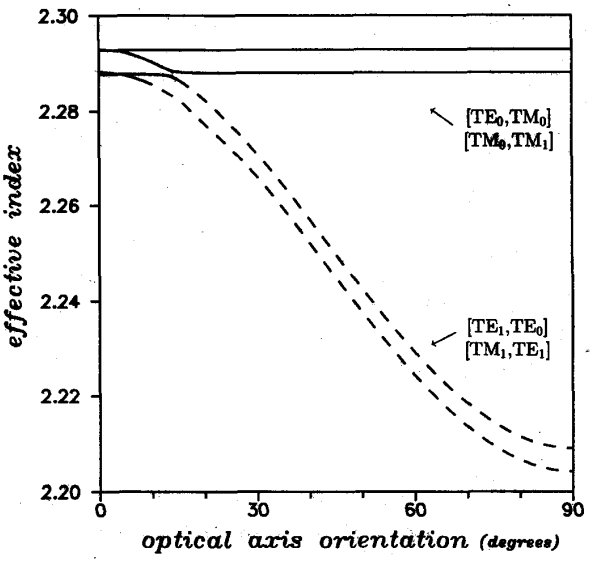

(a)

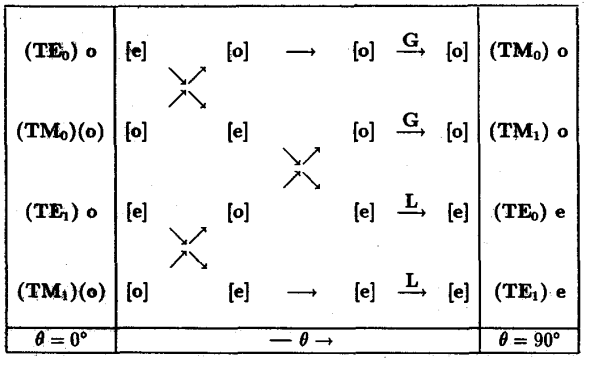

(b)

Fig. 2. (a) Effective index of the hybrid modes guided by G_1 as a function of the optical axis orientation. Continuous lines indicate totally guided modes and dashed lines correspond to leaky modes. (b) $[o]$-$[e]$ diagram for G_1.

undergoes the GLMT. Similarly, the $[TE_1, TE_0]$ mode, which evolves as an $[e]$ -like mode in the neighborhood of $\theta = 0°$ and as an $[o]$-like mode beyond the first NDR, exhibits a second NDR, now with the $[TM_0, TM_1]$ mode. Both modes also invert their nature in the common NDR, so that the first one becomes again an $[e]$-like mode. To sum up, both modes that undergo the GLMT are $[e]$-like modes.

Next, we are going to deal with a waveguide made on a positive birefringent material. In Fig. 3(a) we have plotted the effective indices of the hybrid modes guided by a homogeneous waveguide with various parameters

$$G_2: \begin{cases} n_{of} = 2.1856 & n_{ef} = 2.190 & n_c = 1.0 \\ n_{os} = 2.1834 & n_{es} = 2.1878 & D = 6.0\,\mu\text{m} \end{cases}$$

which correspond to a $LiTaO_3$-based sample. The $[o]$-$[e]$ diagram associated with G_2 is shown in Fig. 3(b). The point is that in this case the GLMT takes place through the $[o]$-like modes. Fig. 3 corresponds to a typical $LiTaO_3$-based waveguide, but if the values of the waveguide parameters are

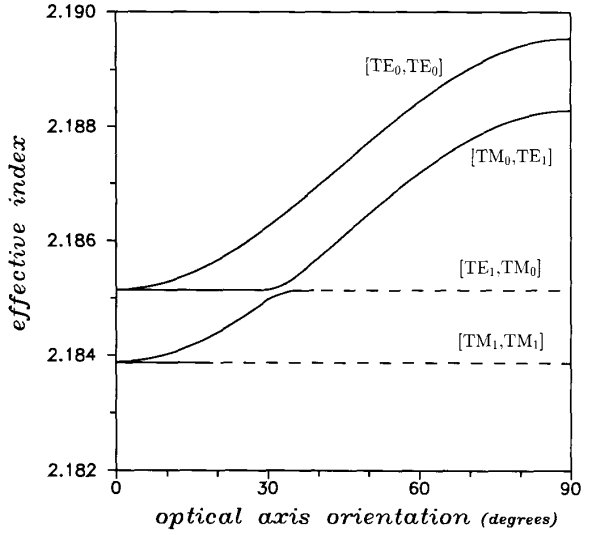

(a)

(TE_0) o	[e]	$\longrightarrow$	[e]	$\longrightarrow$	[e]	$\xrightarrow{G}$ [e]	(TE_0) e
(TM_0)(o)	[o]	$\longrightarrow$	[o]		[e]	$\xrightarrow{G}$ [e]	(TE_1) e
(TE_1) o	[e]	$\longrightarrow$	[e]		[o]	$\xrightarrow{L}$ [o]	(TM_0) o
(TM_1)(o)	[o]	$\longrightarrow$	[o]	$\longrightarrow$	[o]	$\xrightarrow{L}$ [o]	(TM_1) o
$\theta = 0°$			$\longrightarrow \theta \longrightarrow$				$\theta = 90°$

(b)

Fig. 3. (a) Effective index of the hybrid modes guided by G_2 as a function of the optical axis orientation. (b) $[o]$-$[e]$ diagram for G_2.

slightly modified, the ordering of the effective indices of the TE-TM modes with equal order that occurs at $\theta = 0°$ may reverse in relation to the one exhibited by G_2. In this case, the $[o]$-$[e]$ diagram becomes identical to Fig. 2(b), but with interchanged TE-TM and $[o]$-$[e]$ roles.

Finally, Fig. 4 corresponds to a typical proton-exchanged $LiNbO_3$ waveguide, with various parameters

$$G_3: \begin{Bmatrix} n_{of} = 2.2466 & n_{ef} = 2.329 & n_c = 1.0 \\ n_{os} = 2.2866 & n_{es} = 2.2028 & D = 1.5\,\mu\text{m} \end{Bmatrix}$$

Due to the negative increment of the ordinary refractive index ($n_{of} < n_{os}$) that is obtained by the proton exchange technique, this waveguide does not allow guided solutions at $\theta = 0°$ [30]. Likewise, at $\theta = 90°$, only TE guided waves (e-like modes) are allowed. G_3 supports four modes. Both TE_2 and TE_3 modes propagate with $N < n_{os}$; thus, any angular deviation renders them leaky modes. The TE_0 and the TE_1 evolve as $[e]$-like modes when θ decreases from 90°, and both of them become leaky.

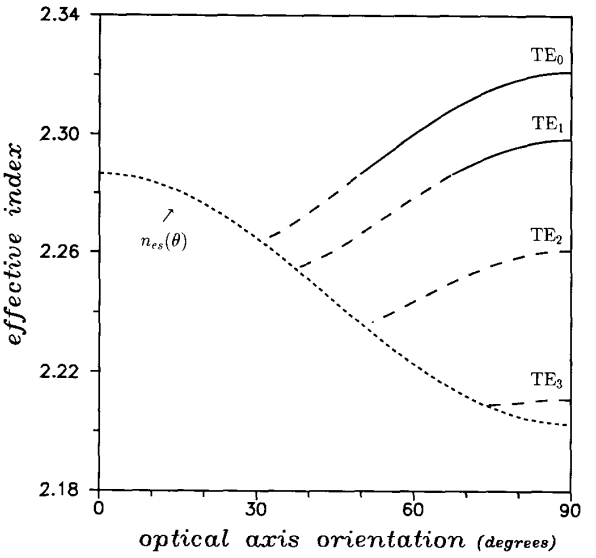

Fig. 4. Effective index of the hybrid modes guided by G_3 as a function of the optical axis orientation. The dotted line stands for the cutoff locus $N = n_{es}(\theta)$.

The $[o]$-$[e]$ diagrams must be interpreted with caution, since the notations of $[o]$-like and $[e]$ -like mode and near-degeneracy region come from somewhat intuitive insights. Near cutoff, the identification of these characteristics on the $\theta - N$ plot is not easy; hence, the corresponding diagrams must be interpreted accordingly. The main usefulness of the $[o]$-$[e]$ diagrams comes from the fact that they summarize the properties of a given waveguide concerning off-axis propagation conditions, so that a great deal of the information can be immediately read off from them.

V. Guided-to-Leaky Mode Transition

The GLMT takes place when one of the ordinary or extraordinary waves forming the hybrid mode reaches its cutoff for total internal reflection, whereas the other remains totally reflected. Thus, two different cases must be distinguished: the cutoff of the ordinary wave and the cutoff of the extraordinary wave. The first case will be referred to as the *ordinary cutoff* (o-cutoff) and the second as the *extraordinary cutoff* (e-cutoff). Next we obtain the expression giving the exact value of the GLMTA in both cases. An alternative approximate procedure based on coupled-mode insights is given in the Appendix.

When the ordinary wave reaches its cutoff for total internal reflection at the film-substrate dielectric boundary, its transversal propagation constant at the substrate vanishes; hence, one has $\gamma_{os} = 0$. Thus, according to (6) we can write

$$o\text{-cutoff} \Rightarrow N = n_{os} \tag{23}$$

Consequently, the transversal propagation constant of the extraordinary wave in the substrate region

$$\gamma_{es}|_{o\text{-cutoff}} = \sqrt{n_{os}^2 - n_{es}^2}\sin\theta_{l,o} \tag{24}$$

Conversely, since here $\hat{c} \cdot \hat{z} = 0$, at the extraordinary cutoff one has $\gamma_{es} = 0$. According to (7), this condition yields

$$e\text{-cutoff} \Rightarrow N = n_{es}(\theta_{l,e}) \tag{25}$$

Hence

$$\gamma_{os}|_{e\text{-cutoff}} = n_{os}\sqrt{\frac{n_{es}^2 - n_{os}^2}{n_{os}^2 \sin^2\theta_{l,e} + n_{es}^2 \cos^2\theta_{l,e}}} \cdot \sin\theta_{l,e} \tag{26}$$

Expressions (24) and (26) lead to the following general conclusion: The ordinary cutoff, taken as partial cutoff, can only occur when considering negative birefringent crystals. The equivalent statement applies for the extraordinary cutoff and positive birefrignent crystals.

A. Ordinary Cutoff

At the ordinary cutoff, the substitution of (23) into the expressions for the coefficients Δ defined in (12), (13) yields

$$\Delta_{oz}|_{o\text{-cutoff}} \sim \frac{1}{\gamma_{os}} \to \infty \tag{27}$$

$$\Delta_{ey}, \Delta_{ez}|_{o\text{-cutoff}} \sim \frac{1}{\gamma_{os}^2} \to \infty \tag{28}$$

These divergences allow us to notably simplify the expression of the eigenvalue equation (19), since only the predominant terms must be retained on it. One arrives simply at

$$\{N_{14} + \gamma_{es} N_{13}\}_{o\text{-cutoff}} = 0 \tag{29}$$

When all media forming the waveguide are isotropic, $\gamma_{os} = 0$ implies $\gamma_{es} = 0$. In this case, taking into account also the properties of the characteristic matrix of an isotropic film, (29) becomes

$$\underbrace{\left[T_{11} + j\frac{n_c^2}{\eta\gamma_c} T_{12}\right]}_{\text{TM}} \quad \underbrace{\left[T_{43} + j\frac{\gamma_c}{\eta} T_{33}\right]}_{\text{TE}} = 0 \tag{30}$$

which is the cutoff condition for TE and TM modes [31].

B. Extraordinary Cutoff

At the extraordinary cutoff the coefficients Δ write assuming that

$$\Delta_{ey}|_{e-\text{cutoff}} = -\frac{n_{os}^2 \sin^2\theta_{l,e} + n_{es}^2 \cos^2\theta_{l,e}}{(n_{es}^2 - n_{os}^2)\sin\theta_{l,e}\cos\theta_{l,e}} \tag{31}$$

$$\Delta_{es}|_{e-\text{cutoff}} = -j\frac{n_{es}}{\sqrt{n_{es}^2 - n_{os}^2 \cos\theta_{l,e}}} \tag{32}$$

$$\Delta_{ez}|_{o\text{-cutoff}} = 0 \tag{33}$$

$n_{os} \neq n_{es}$. The substitution of (31)–(33) into (19) yields

$$\{(1 - \Delta_{ox}\Delta_{ey})N_{24} + \Delta_{ey}(N_{34} - \Delta_{ey}N_{14}) + \gamma_{os}(N_{23} + \Delta_{ey}N_{12})\}_{e\text{-cutoff}} = 0 \tag{34}$$

C. Allowed Values of θ_l

Generally speaking, the GLMTA can take all possible values in the range $[0°, 90°]$. Nevertheless, for typical waveguides, θ_l is bounded by a maximum or minimum value, characteristic of each waveguide. The obtainment of this bounding value runs as follows. Since we are looking for either totally and leaky guided solutions, power flow must be parallel to the film-substrate interface at least for one of the two kinds of waves, ordinary and extraordinary, forming the hybrid modes. For the ordinary waves this condition implies

$$n_{of} > N > n_{os} \tag{35}$$

whereas for the extraordinary waves it writes

$$n_{ef}(\theta) > N > n_{es}(\theta) \tag{36}$$

with $n_{ef}(\theta)$ being defined as in (8). At $\theta = 0°$, (36) reduces to (35), whereas at $\theta = 90°$ one has $n_{ef,es}(90°) = n_{ef,es}$, and (36) becomes identical to (35) but for the extraordinary refractive indices. There upon, since for the waveguides such as G_1, one has $n_{of} > n_{os} > n_{es}$, and the o-cutoff occurs at $N = n_{os}$, the maximum value that can be reached by $\theta_{l,o}$ comes from the equality $n_{ef}(\theta_{lm,o}) = n_{os}$. This condition yields

$$\theta_{lm,o} = \sin^{-1}\left\{\frac{n_{ef}}{n_{os}}\left(\frac{n_{of}^2 - n_{os}^2}{n_{of}^2 - n_{ef}^2}\right)^{1/2}\right\} \tag{37}$$

The same expression holds for G_3, although now $\theta_{lm,o}$ stands for the minimum allowed value of $\theta_{l,o}$. On the other hand, when considering waveguides made on positive birefringent crystals such as G_2, one has $n_{ef} > n_{es} > n_{of} > n_{os}$. Therefore, since the e-cutoff occurs when $N = n_{es}(\theta_{l,e})$, the maximum value which can be reached by $\theta_{l,e}$ verifies $n_{es}(\theta_{lm,e}) = n_{of}$. Hence, one gets

$$\theta_{lm,e} = \sin^{-1}\left\{\frac{n_{es}}{n_{of}}\left(\frac{n_{of}^2 - n_{os}^2}{n_{es}^2 - n_{os}^2}\right)^{1/2}\right\} \tag{38}$$

In view of (37) and (38), we notice that θ_{lm} depends on the film and substrate refractive indexes, but it is independent of the cover refractive index, as well as on the ratio D/λ. Also, $\theta_{lm,o}$ ($\theta_{lm,e}$) does not depend on n_{es} (n_{ef}), whereas $\theta_{lm,e}$ ($\theta_{lm,o}$) does.

VI. Discussion

The behavior of the GLMTA as a function of the various waveguide parameters has been investigated by solving (29) and (34). The outcome for typical structures is shown in Figs. 5–10.

In Fig. 5 we have plotted θ_l as a function of the ratio D/λ, for a G_1-like waveguide. The curves in the plot correspond to the different hybrid modes guided by the structure for each value of D/λ. As this ratio grows, not only the number of TE-TM-allowed guided modes at $\theta = 0, 90°$ increases, but the nature of the hybrid modes modifies as well, since leaky modes convert into totally guided ones. Both effects occur with very small variations of D/λ; hence, very sharp

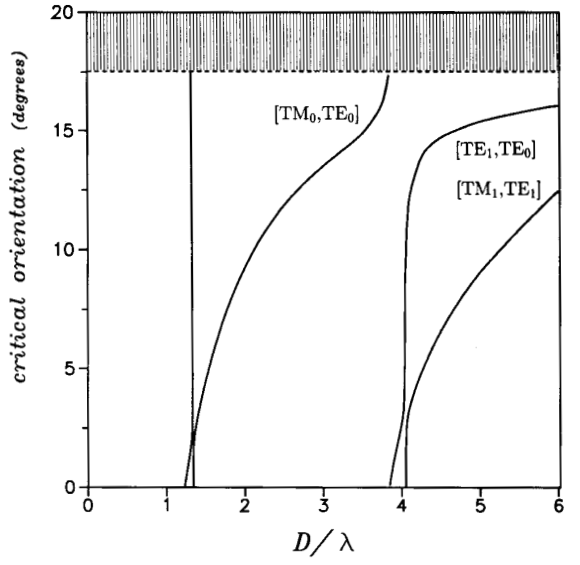

Fig. 5. Guided-to-leaky mode transition angle for the hybrid modes guided by G_1, as a function of the λ-scaled waveguide thickness. Shaded region corresponds to the guided-to-radiated mode transition. Here and in Fig. 6, the unlabelled curve corresponds to a mode which is cutoff at $\theta = 0°, 90°$.

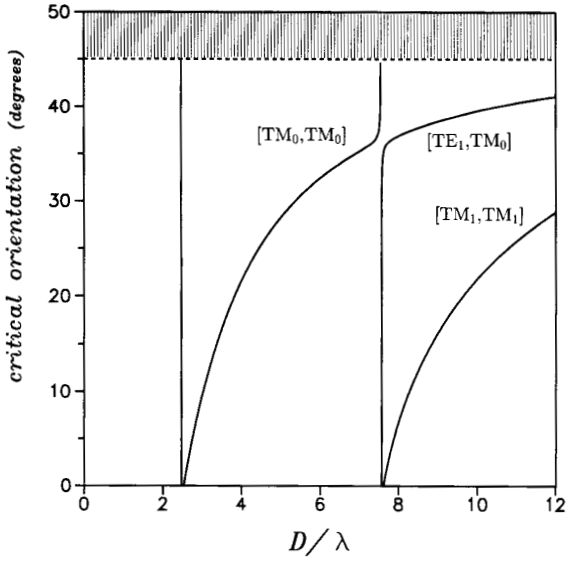

Fig. 6. Same as in Fig. 5, but for G_2.

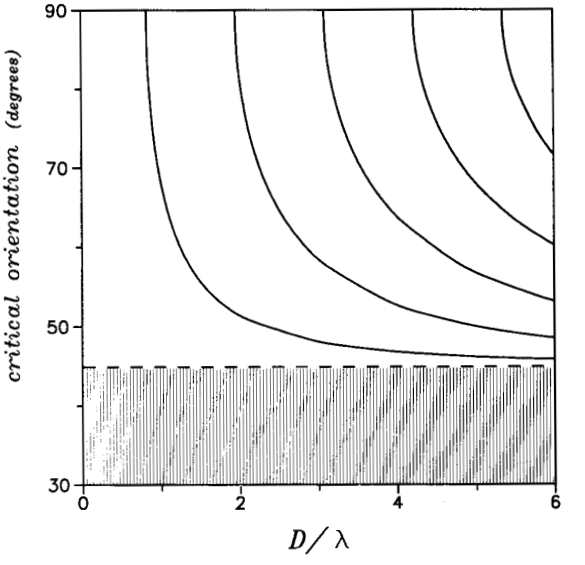

Fig. 7. Same as in Fig. 5, but for G_3. Here shaded region indicates forbidden values. From left to right: TE_0–TE_4, at $\theta = 90°$.

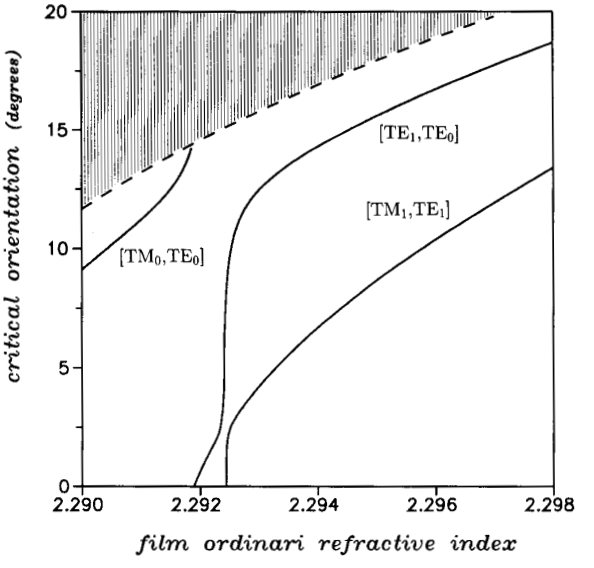

Fig. 8. Guided-to-leaky mode transition angle for the hybrid modes guided by G_1, as a function of the film ordinary refractive index.

changes in θ_l take place. Higher order TE-TM modes become allowed at given critical thicknesses, the cutoff thicknesses, whereas the leaky-to-guided mode transformation is a gradual but fast process as a function of D/λ. The cutoff thicknesses of the TE-TM modes taking place at $\theta = 0, 90°$ are given by simple expressions [4]. In the neighborhood of these cutoff thicknesses, some roots of (29) yielding $\theta_{l,o} > \theta_{lm,o}$ appear. These roots correspond to the a total cutoff and evolve very fast from $\theta_{lm,o}$ to 90° as a function of D/λ. The same comments hold as well for the curves in Fig. 6, which corresponds to a G_2-like waveguide. Finally, Fig. 7 corresponds to a proton-exchanged sample such as G_3. In this plot, $\theta_{l,o}$ starts at 90°, and decreases assymptotically toward $\theta_{lm,o}$ when D/λ grows.

In order to display the behavior of θ_l as a function of the various refractive indices involved, we have chosen a representative example for each case. The obtained results have been plotted in Figs. 8–10. As above, the global pattern of the plots, including fast variations of θ_l near $\theta_l = 0°$ and $\theta_l = \theta_{lm}$, and multiple values of θ_l with a fixed value of n_{of} or n_{ef}, comes from both the greater number of allowed modes

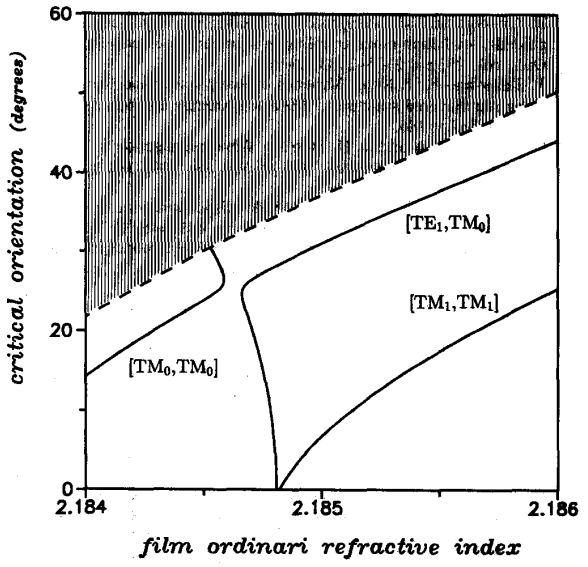

Fig. 9. Same as in Fig. 8, but for G_2.

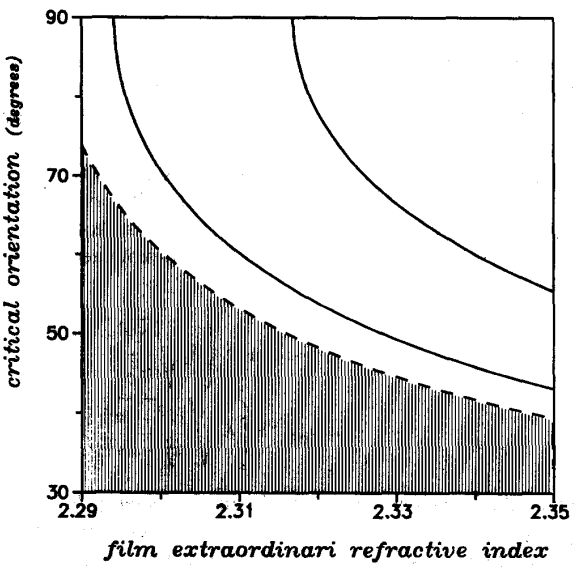

Fig. 10. Guided-to-leaky mode transition angle for hybrid modes guided by G_3, as a function of the film extraordinary refractive index. From left to right: TE_0, TE_1, at $\theta = 90°$.

and the leaky-to-guided mode transformation, which take place as the film refractive indexes increase. The salient point of the plots that must be emphasized is the large shifts exhibited by θ_l with very small increments in the film refractive indexes. Typically, an increment of about $\Delta n \sim 0.001$ yields $\Delta\theta_l \sim 1°$, and the larger the value of θ_{lm}, the larger $\Delta\theta_l$. Away from the cutoff point of the TE-TM modes, θ_l depends almost linearly with n_{of}, in the case of G_1 and G_2, and with n_{ef}, in the case of G_3. The values of the film refractive indices can be reasonably controlled in the fabrication process, so that θ_l can be approximately tuned to a desired value within a wide range.

Modification of the film refractive index by modifying the temperature of the guiding film, for instance by optical absorption processes, seems to be an interesting possibility. Typically, the thermally induced bulk refractive index variations at room temperature amount to $dn/dT \approx 10^{-4}-10^{-5}$°C for $LiNbO_3$, $LiTaO_3$, $LiIO_3$, or $BaTiO_3$ [32], [33], and as a rule dn_e/dT is larger than dn_o/dT. In this line, it must be noted that the variations of θ_l caused by an increment of a film refractive index are practically counterbalanced by the same increase of the corresponding substrate refractive index. Therefore, in order to obtain a notable modification on the value of θ_l, an asymmetrical response on the film and substrate refractive indices to a temperature change should be desirable. Photoabsorption heating caused by totally guided modes would verify this requirement, since most of the guided wave power travels into the film region.

VII. Concluding Remarks

We have investigated the guided-to-leaky hybrid mode transition in planar optical waveguides made on uniaxial crystals like $LiNbO_3$ or $LiTaO_3$. Two different guided-to-leaky transitions have been identified, namely the *ordinary cutoff* and the *extraordinary cutoff*, which respectively occur when considering negative and positive birefringent materials, and analytical, yet transcendental, expressions yielding the critical optical axis orientation above which the totally guided hybrid modes become leaky, θ_l, have been obtained. The dependence of θ_l on the waveguide thickness and on the film and substrate refractive indices has been investigated, and fast variations have been found. Concerning the cover refractive index, θ_l is nearly insensitive to the particular value of this parameter, provided that a low-index medium is deposited over the guiding film, but large variations arise again when considering nearly symmetrical structures.

Actually, in a result opposite that of the proton exchange technique, titanium indiffusion yields inhomogeneous waveguides. In order to take into account this fact, graded-index versions of G_1 and G_2, with a gaussian profile in both the ordinary and extraordinary refractive indexes, have been analyzed. Numerics indicate that the graded-index nature of the guiding film renders θ_l to different values than its step-index counterpart. For instance, concerning the $[TE_1, TE_0]$ hybrid mode guided by G_1, $\theta_{l,o} \approx 15.1°$ for a step-index film, whereas $\theta_{l,o} \approx 12.8°$ in the graded-index case. We have made no attempt to do extensive calculations for the graded-index waveguides, but in representative cases, no significant differences have been found in the behavior of θ_l with the involved waveguide parameters, in relation to the step-index case.

Potential new interesting applications of the guided-to-leaky mode transition come from the switching properties associated with the large variations of θ_l caused by changes in the refractive indices involved. In suitable conditions, leaky modes exhibit large losses [18]–[24], [26], [30]; thus, sharp switching characteristics will arise. Success depends on the possibility of tuning the value of this critical angle through the waveguide parameters, either by controlling the fabrication procedure or by means of dynamical processes. Thermally induced refractive index changes caused by photoabsorption seem to be an exciting possibility to be investigated [34].

APPENDIX

In this appendix we briefly outline an approximate procedure, based on the coupled-mode approach, to obtain the GLMTA. Key points run as follows (see, e.g., [8]). Since $\epsilon_{xy} \ll \epsilon_{yy}, \epsilon_{zz}$, the hybrid modes guided by G_1–G_3 can be approximately regarded as weakly perturbed pure TE and TM modes. TE waves would render to $[e]$-like modes, whereas TM waves would correspond to the $[o]$-like ones. Accordingly, the eigenvalue equation (19) can be approximated by the well-known expression

$$k_o D\sqrt{n_f^2 - N^2} = m\pi + \tan^{-1}\left\{\delta_1\sqrt{\frac{N^2 - n_c^2}{n_f^2 - N^2}}\right\} + \tan^{-1}\left\{\delta_2\sqrt{\frac{N^2 - n_s^2}{n_f^2 - N^2}}\right\} \quad (39)$$

where the integer m stands for the mode operator, $\delta_{1,2;\mathrm{TE}} = 1, \delta_{1;\mathrm{TM}} = n_f^2/n_c^2$, and $\delta_{2;\mathrm{TM}} = n_f^2/n_s^2$. According to (2), the appropriate substrate and film refractive indexes write $n^2 = n_o^2\cos^2\theta + n_e^2\sin^2\theta$ for TE modes, and $n^2 = n_o^2$ in the TM case. Finally, the ordinary cutoff takes place at $N_{\mathrm{TE}} = n_{os}$, whereas the extraordinary one comes from the condition $N_{\mathrm{TM}} = n_{es}(\theta)$. The outcome expressions render once again transcendental, but easier, equations than (29) and (34), with their numerical roots exhibiting an excellent agreement with the exact solutions. The best fit occurs for G_3-like samples and also for single-mode G_1, G_2-like waveguides.

REFERENCES

[1] R. R. A. Syms, "Advances in channel waveguide lithium niobate integrated optics," *Opt. Quantum Electron.*, vol. 20, pp. 189–213, 1988.

[2] L. Thylén, "Integrated optics in $LiNbO_3$: Recent developments in devices for telecommunications," *J. Lightwave Technol.*, vol. LT-6, pp. 847–861, 1988.

[3] J. v Ctyroký, R. Göring, J. Janta, W. Karthe, A. Rasch, M. Rotttschalk, and J. Schröfel, "Integrated Electrooptic Modulators and Switches in $LiNbO_3$," *Kybernetika,* vol. 26, pp. 171–190, 1990.

[4] T. K. Gaylord and A. Knoesen, "Passive integrated optical anisotropy-based devices," *J. Mod. Opt.*, vol. 35, pp. 925–946, 1988.

[5] A. Neyer and W. Sohler, "High-speed cutoff modulator using Ti-diffused $LiNbO_3$ channel waveguide," *Appl. Phys. Lett.*, vol. 35, pp. 256–258, 1979.

[6] T. Findakly, B. Chen, and D. Booher, "Single-mode integrated-optical polarizers in $LiNbO_3$ and glass waveguides," *Opt. Lett.*, vol. 8, pp. 641–643, 1983.

[7] J. J. Veselka and G. A. Bogert, "Low-loss TM-pass polarizer fabricated by proton exchange for Z-cut Ti: $LiNbO_3$ waveguides," *Electron. Lett.*, vol. 23, pp. 37–38, 1987.

[8] S. Yamamoto and Y. Okamura, "Guided-radiation mode interaction in off-axis propagation in anisotropic optical waveguides with application to direct-intensity modulators," *J. Appl. Phys.*, vol. 50, pp. 2555–2564, 1979.

[9] S. T. Kirsch *et al.*,"Semileaky thin-film optical isolator," *J. Appl. Phys.*, vol. 52, pp. 3190–3199, 1981.

[10] D. Marcuse, "Electrooptic coupling between TE and TM modes in anisotropic slabs," *IEEE J. Quantum Electron.*, vol. QE-11, pp. 759–767, 1975.

[11] Y.-K. Lee and S. Wang, "Electrooptic guided-to-unguided mode converter," *IEEE J. Quantum Electron.*, vol. QE-12, pp. 273–281, 1976.

[12] Y. Okamura, K. Kitatani, and S. Yamamoto, "Electrooptic leaky anisotropic waveguides using nematic liquid crystal overlayers," *J. Lightwave Technol.*, vol. LT-2, pp. 292–295, 1984.

[13] H. Onodera, I. Awai, M. Nakajima, and J. Ikenoue, "Light intensity modulation based on guided-to-radiation mode coupling in heterostructure waveguides," *Appl. Opt.*, vol. 23, pp. 118–123, 1984.

[14] H. Onodera and M. Nakajima, "High-efficiency light modulator using guided-to-radiation mode coupling in a graded-index waveguide," *Appl. Opt.*, vol. 25, pp. 2175–2183, 1986.

[15] T. Tamir and F. Y. Kou, "Varieties of leaky waves and their excitation along multilayered structures," *IEEE J. Quantum Electron.*, vol. QE-22, pp. 544–551, 1986.

[16] D. P. Gia Russo and J. H. Harris, "Wave propagation in anisotropic thin-film optical waveguides," *J. Opt. Soc. Am.*, vol. 63, pp. 138–145, 1973.

[17] W. K. Burns and J. Warner, "Mode dispersion in uniaxial optical waveguides," *J. Opt. Soc. Am.*, vol. 64, pp. 441–446, 1974.

[18] J. \v Ctyroký and M. Cada, "Guided and semileaky modes in anisotropic waveguides of the $LiNbO_3$ type," *Opt. Commun.*, vol. 27, pp. 353–357, 1978.

[19] K. Yamanouchi, T. Kamiya, and K. Shibayama, "New leaky surface waves in anisotropic metal-diffused optical waveguides," *IEEE Trans. Microwave Theory Tech.*, vol. MTT-26, pp. 298–304, 1978.

[20] D. Marcuse and I. P. Kaminow, "Modes of a symmetric slab optical waveguide in birefringent media. Part II: Slab with a coplanar optical axis," *IEEE J. Quantum Electron.*, vol. QE-15, pp. 92–101, 1979.

[21] S. K. Sheem, W. K. Burns, and A. F. Milton, "Leaky-mode propagation in Ti-diffused $LiNbO_3$ and $LiTaO_3$ waveguides," *Opt. Lett.*, vol. 3, pp. 76–78, 1978.

[22] W. K. Burns, S. K. Sheem, and A. F. Milton, "Approximate calculation of leaky-mode loss coefficient for Ti-diffused $LiNbO_3$ waveguides," *IEEE J. Quantum Electron.*, vol. QE-15, pp. 1282–1289, 1979.

[23] J. \v Ctyroký and M. Cada, "Generalized WKB method for the analysis of light propagation in inhomogeneous anisotropic optical waveguides," *IEEE J. Quantum Electron.*, QE-17, pp. 1064–1070, 1981.

[24] M. Koshiba, H. Kumagami, and M. Suzuki, "Finite-element solution of planar arbitrarily anisotropic diffused optical waveguides," *J. Lightwave Technol.*, vol. LT-3, pp. 773–778, 1985.

[25] A. Knoesen, T. K. Gaylord, and M. G. Moharam, "Hybrid guided modes in uniaxial dielectric planar waveguides," *J. Lightwave Technol.*, vol. LT-6, pp. 1083–1104, 1988.

[26] L. Torner, F. Canal, and J. Hernandez-Marco, "Leaky modes in multilayer uniaxial optical waveguides," *Appl. Opt.*, vol. 29, pp. 2805–2814, 1990.

[27] D. W. Berreman, "Optics in stratified and anisotropic media: 4×4-matrix formalism," *J. Opt. Soc. Amer.*, vol. 62, pp. 502–510, 1972.

[28] M. O. Vassell, "Structure of optical guided modes in planar multilayers of optically anisotropic materials," *J. Opt. Soc. Amer.*, vol. 64, pp. 166–173, 1974.

[29] H. Wöhler, G. Haas, M. Fritsch, and D. A. Mlynski, "Faster 4×4 matrix method for uniaxial inhomogeneous media," *J. Opt. Soc. Amer. A.*, vol. 5, pp. 1554–1557, 1988.

[30] J. Ctyroký, "Light propagation in proton-exchanged $LiNbO_3$ waveguides," *J. Opt. Commun.*, vol. 5, pp. 16–19, 1984.

[31] L. Torner, F. Canal, and J. Hernandez-Marco, "Cutoff behaviour of graded-index slab waveguides," *Opt. Quantum Electron.*, vol. 21, pp. 451–462, 1989.

[32] R. C. Miller and A. Savage, "Temperature dependence of the optical properties of ferroelectric $LiNbO_3$ and $LiTaO_3$," *Appl. Phys. Lett.*, vol. 9, pp. 169–171, 1966.

[33] D. W. Rush, B. M. Dugan, and G. L. Burdge, "Temperature-dependent index-of-refraction changes in $BaTiO_3$," *Opt. Lett.*, vol. 16, pp. 1295–1297, 1991.

[34] I. C. Khoo and P. Zhou, "Dynamics of switching total internal reflection to transmission in dielectric-cladded nonlinear film," *J. Opt. Soc. Amer. B,* vol. 6, pp. 884–888, 1989.

Lluís Torner, photograph and biography not available at the time of publication.

Jaume Recolons, photograph and biography not available at the time of publication.

Juan P. Torres, photograph and biography not available at the time of publication.